Latest developments from xFitter

Ivan Novikov
on behalf of xFitter developers team
2019-09-17

Outline

- Analyses being prepared
  - PDF Profiling Using the Forward-Backward Asymmetry in Neutral Current Drell-Yan Production
  - Probing the strange content of the proton with charm production in charged current at LHeC
  - Parton Distribution Functions of the Charged Pion Within The `xFitter` Framework
- Development of `xFitter` code

PDF Profiling Using the Forward-Backward Asymmetry in Neutral Current Drell-Yan Production (arxiv:1907.07727)

How will new $A^*_{\rm FB}$ data on neutral-current Drell-Yan process from the LHC improve determinations of PDFs?

$$A^*_{\rm FB} = \frac{\sigma_F - \sigma_B}{\sigma_F + \sigma_B}, \quad \sigma_F = \sigma[\cos\theta > 0], \quad \sigma_B = \sigma[\cos\theta < 0],$$

where θ is the angle between the incoming quark and the outgoing lepton in the Collins-Soper frame.

Perform profiling for differnt PDF sets: CT14nnlo[1], NNPDF3.1nnlo (Hessian set)[2], ABMP16nnlo[3], HERAPDF2.0nnlo (EIG)[4], and MMHT2014nnlo[5]

$$\frac{\mathrm{d}^3\sigma}{dM_{\ell\ell}dy_{\ell\ell}d\cos\theta^*} = \frac{\pi\alpha^2}{3M_{\ell\ell}s}\sum_q P_q\left[f_q(x_1,Q^2)f_{\bar{q}}(x_2,Q^2) + f_{\bar{q}}(x_1,Q^2)f_q(x_2,Q^2)\right]$$

$$\begin{aligned}P_q &= e_\ell^2 e_q^2(1+\cos^2\theta^*)\\ &+ \frac{2M_{\ell\ell}^2(M_{\ell\ell}^2 - M_Z^2)}{\sin^2\theta_W\cos^2\theta_W\left[(M_{\ell\ell}^2 - M_Z^2)^2 + \Gamma_Z^2 M_Z^2\right]}(e_\ell e_q)\left[v_\ell v_q(1+\cos^2\theta^*) + 2a_\ell a_q\cos\theta^*\right]\\ &+ \frac{M_{\ell\ell}^4}{\sin^4\theta_W\cos^4\theta_W\left[(M_{\ell\ell}^2 - M_Z^2)^2 + \Gamma_Z^2 M_Z^2\right]}[(a_\ell^2+v_\ell^2)(a_q^2+v_q^2)(1+\cos^2\theta^*)\\ &+ 8a_\ell v_\ell a_q v_q\cos\theta^*],\end{aligned}$$

Terms other than those linear in $\cos\theta^*$ cancel in A^*_{FB}, and the dominant contribution is the γZ interference term.

Therefore, we expect $A^*_{\mathrm{FB}}$to be sensitive to
$e_\ell a_\ell[e_u a_u u_V(x,Q^2) + e_d a_d d_V(x,Q^2)] \propto \frac{2}{3}u_V(x,Q^2) + \frac{1}{3}d_V(x,Q^2)$
This is complementary to lepton charge asymmetry Drell-Yan data, which is most sensitive to $u_v - d_v$

Pseudodata was generated in bins of dilepton mass $M_{\ell\ell}$ from 45 GeV to 200 GeV with step 2.5 GeV (62 bins), and with different dilepton rapidity $|y_{\ell\ell}|$ cuts, from $|y_{\ell\ell}| = 0$ to $|y_{\ell\ell}| = 2.5$ with step 0.5.
The statistical uncertainty of the pseudodata was based on 3 values for integrated luminosity:

- $L = 30\ \text{fb}^{-1}$,
- $L = 300\ \text{fb}^{-1}$ (end of Run 3),
- $L = 3000\ \text{fb}^{-1}$ (end of HL-LHC).

This estimate of statistical uncertainty included a factor of ~ 0.2 for detector acceptance and efficiency.
Predictions at LO and NLO were obtained using MadGraph5_aMC@NLO[6], APPLgrid[7], and aMCfast[8] packages, and with an independent analytical code at LO.

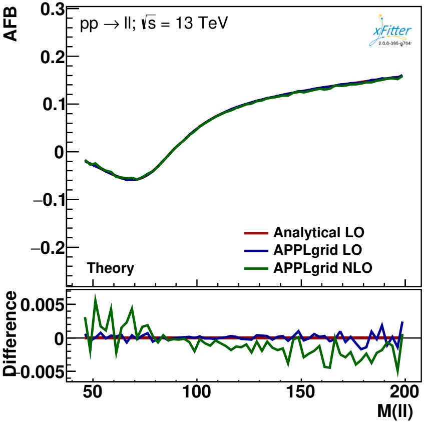

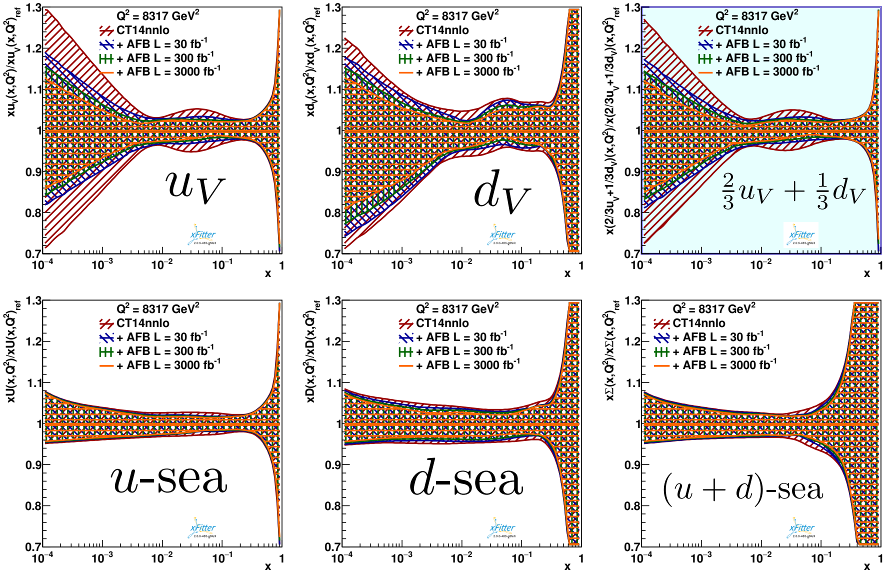
Q² = 8317 GeV²
CT14nnlo
+ AFB L = 30 fb⁻¹
+ AFB L = 300 fb⁻¹
+ AFB L = 3000 fb⁻¹
u_V
d_V
$\frac{2}{3}u_V + \frac{1}{3}d_V$
u-sea
d-sea
$(u+d)$-sea
xFitter
x

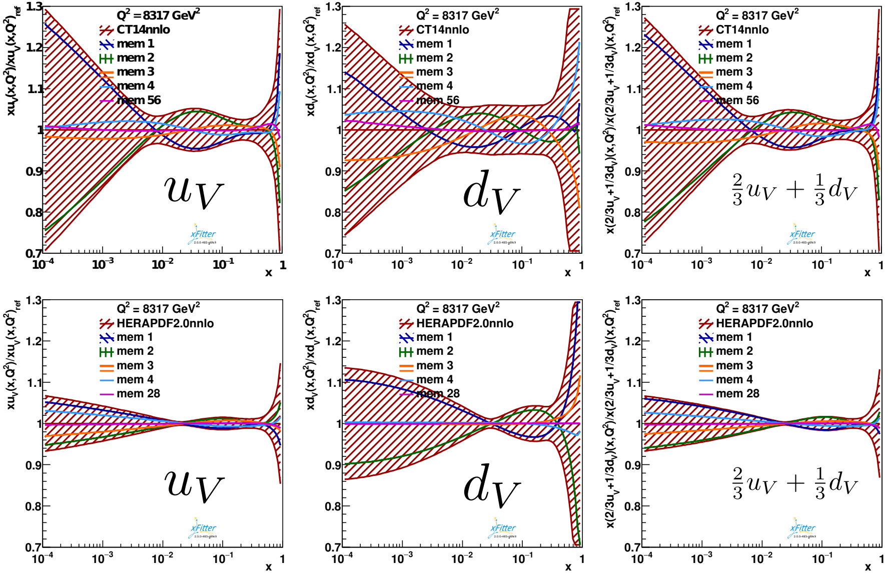
Q^2 = 8317 GeV^2
CT14nnlo
mem 1
mem 2
mem 3
mem 4
mem 56
HERAPDF2.0nnlo
mem 28
u_V
d_V
$\frac{2}{3}u_V + \frac{1}{3}d_V$
xu_v(x,Q^2)/xu_v(x,Q^2)_ref
xd_v(x,Q^2)/xd_v(x,Q^2)_ref
x(2/3u_v+1/3d_v)(x,Q^2)/x(2/3u_v+1/3d_v)(x,Q^2)_ref
x
xFitter

Probing the strange content of the proton with charm production in charged current at LHeC (arxiv:1907.01014)

1. How can future data on charm pruduction in charged-current DIS at the LHeC constrain strange-quark PDF?
2. What is the difference in predictions for different heavy flavor schemes?

Heavy-flavor schemes:

FFNS A
: 3 flavors in both PDFs and α_S evolution. Heavy flavors (charm) appear in matix elements only.
PDF sets: `ABMP16`[9], `HERAPDF2.0 FF3A`[4]

FFNS B
: 3 flavors in PDFs, but variable number of active flavors in α_S evolution. At NLO same matrix elements as in `FFNS A`.
PDF sets: `HERAPDF2.0 FF3B`[4]

FONLL-B
: (VFNS) Variable number of active flavors both in PDFs and in α_S evolution, neglecting masses. Fixed-order-next-to-leading massive matrix elements.
PDF sets: `NNPDF3.1`[2]

Predictions for each scheme are obtained with associated PDF sets and theory parameters. All calculations and PDF sets are at NLO.

Feynman diagrams in VFNS and in FFNS

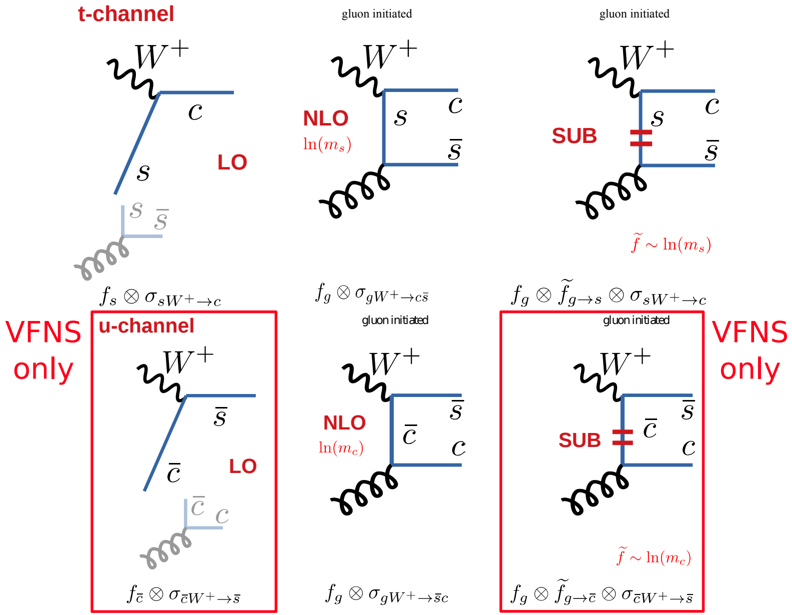

Predictions are different at large Q^2 and high-x

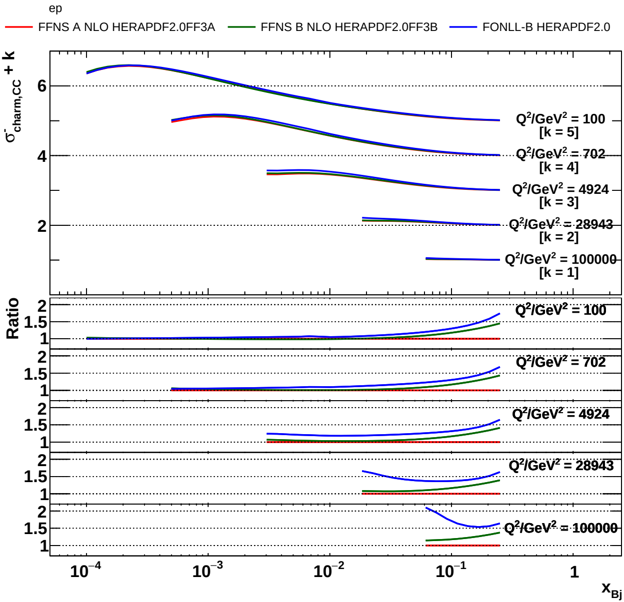

Pseudodata was generated with $L = 100\ \text{fb}^{-1}$ and electron polarisation $P = -0.8$

Restrict profiling to points with $\Delta_{\text{scheme}} < \Delta_{\text{PDF}}$

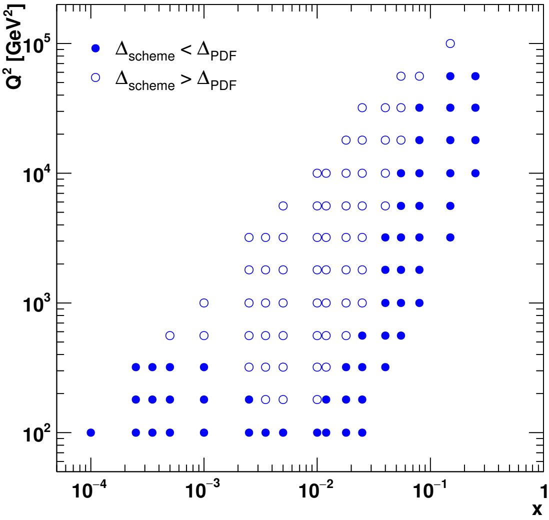

Profiling ABMP16

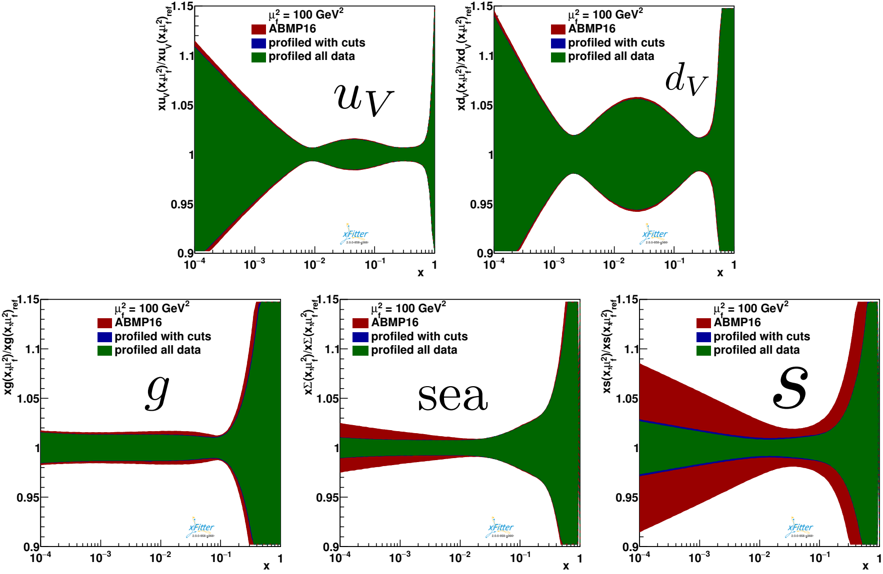

Profiling NNPDF3.1

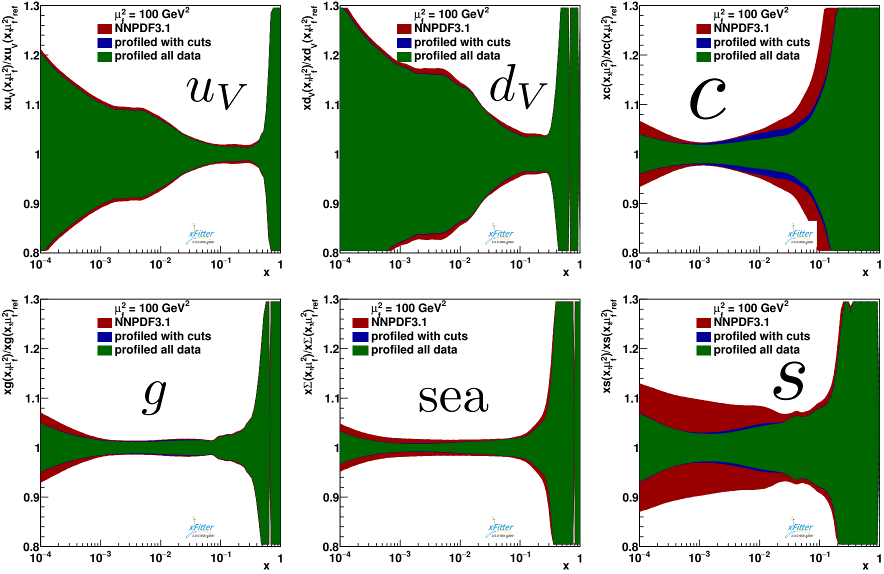

Parton Distribution Functions of the Charged Pion Within The `xFitter` **Framework** (will be uploaded to arxiv in a few weeks)
A Next-to-leading order extraction of PDFs of charged pion from Drell-Yan and prompt photon production data.
E615[10] and NA10[11] experiments studied Drell-Yan dimuon production with a negative pion beam on a tungsten target:

$$\pi^{-}\,{}^{184}_{74}\mathrm{W} \to \mu^{+}\mu^{-}X$$

The WA70[12] experiment studied prompt photon production with beams of negative and positive pions and a proton target:

$$\pi^{\pm}p \to \gamma X$$

In comparison to the prompt photon data, the Drell-Yan data is more precise, but is only sensitive to valence-quark PDFs. The prompt photon data has some sensitity to sea and gluon, but also has larger uncertainties.
Predictions are obtained using APPLgrid[7], grids were generated using MCFM[13]. QCDNUM[14] library is used for DGLAP evolution. Nuclear PDF set nCTEQ15[15] was used for target PDFs.

To parameterize PDFs of π^-, assume at the initial scale $Q_0^2 = 1.9$ GeV^2 charge symmetry: $d = \bar{u}$, and $SU(3)$-symmetric sea: $u = \bar{d} = s = \bar{s}$.

$$v := (d - \bar{d}) - (u - \bar{u}), \qquad xv(x) = A_v x^{B_v}(1-x)^{C_v}(1 + D_v x^{\frac{5}{2}}),$$
$$S := 2u + 2\bar{d} + s + \bar{s} = 6u, \qquad xs(x) = A_S x^{B_S}(1-x)^{C_S},$$
$$g := g, \qquad xg(x) = A_g x^{B_g}(1-x)^{C_g}.$$

The A_v and A_g parameters are determined by the sum rules:

$$\int_0^1 v(x)\mathrm{d}x = 2, \qquad \int_0^1 x(v(x) + S(x) + g(x))\mathrm{d}x = 1.$$

Initial fits failed to determine all sea and gluon parameters simultaneously, so we fixed $C_s = 8$, $C_g = 5$.

Extracted pion PDFs

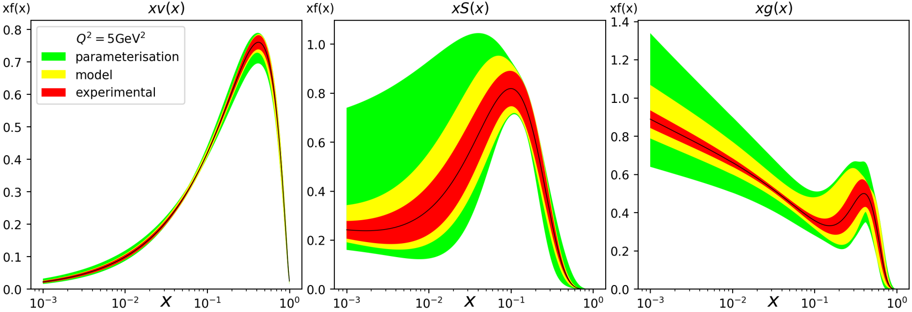

$$\frac{\chi^2}{N_{\mathrm{DoF}}} = \frac{474}{373} = 1.27$$

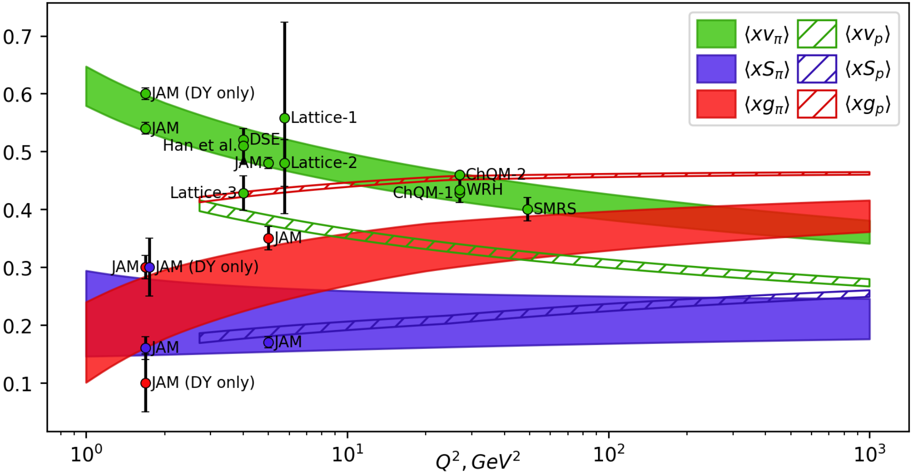

We evaluate fractions of pion's momentum carried by valence quarks, sea quarks, and gluon, as a function of factorization scale Q^2, and compare them to predictions of theoretical models, results of lattice QCD calculations, and results of fits by other groups (See legend in backup section)

New bugfix release `xFitter` **2.0.1 "OldFashioned"**, available on https://xfitter.org

Overview of improvements in `xFitter` 2.2 (unreleased, experimental)

- New flexible and modular fit architecture
  - Support for multiple PDFs in the same fit
  - Easy way to provide parameterisations as a formula in steering file
- Improved LHAPDF support, for both export and import
- Moving from `Fortran` `NAMELIST`-based steering to `YAML`
- Partial support of `Ceres` minimizer, as an alternative to `MINUIT`
- Changing build system from `autotools` to `CMake`

Available on gitlab:
https://gitlab.cern.ch/fitters/xfitter/

Thank you for your attention!

Backup

Label	$\langle xv \rangle$	$\langle xS \rangle$	$\langle xg \rangle$	Q^2 (GeV^2)
JAM[16]	0.54 ± 0.01	0.16 ± 0.02	0.30 ± 0.02	1.69
JAM (DY)	0.60 ± 0.01	0.30 ± 0.05	0.10 ± 0.05	1.69
this work	0.58 ± 0.04	0.21 ± 0.07	0.21 ± 0.07	1.69
Lattice-3[17]	0.428 ± 0.030			4
SMRS[18]	0.40 ± 0.02			4
Han et al.[19]	0.428 ± 0.03			4
DSE[20]	0.52			4
this work	0.52 ± 0.04	0.21 ± 0.06	0.27 ± 0.06	4
JAM	0.48 ± 0.01	0.17 ± 0.01	0.35 ± 0.02	5
this work	0.51 ± 0.04	0.21 ± 0.06	0.28 ± 0.06	5
Lattice-1[21]	0.558 ± 0.166			5.76
Lattice-2[22]	0.48 ± 0.04			5.76
this work	0.50 ± 0.04	0.21 ± 0.06	0.28 ± 0.06	5.76
WRH[23]	0.434 ± 0.022			27
ChQM-1[24]	0.428			27
ChQM-2[25]	0.46			27
this work	0.45 ± 0.03	0.21 ± 0.05	0.33 ± 0.06	27
SMRS[18]	0.49 ± 0.02			49
this work	0.43 ± 0.03	0.21 ± 0.05	0.35 ± 0.04	49

AFB profiling with different rapidity cuts

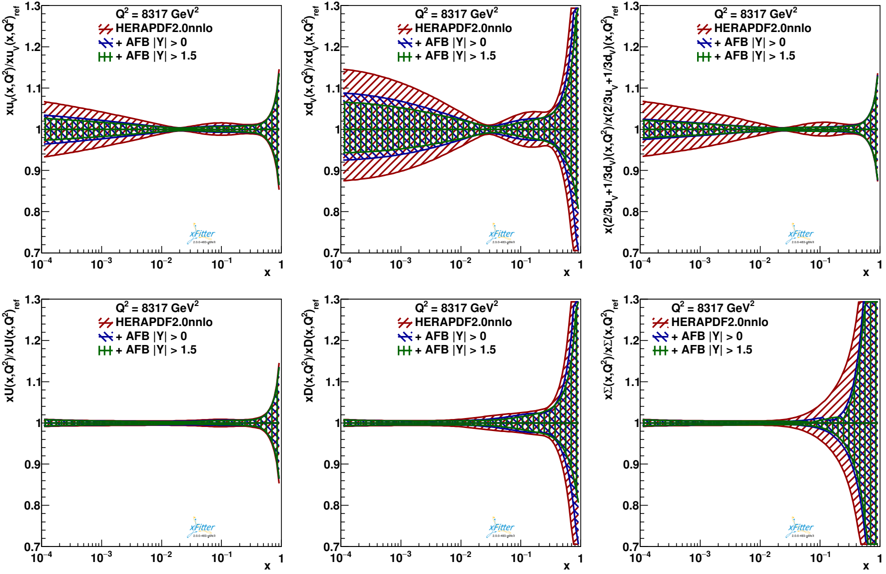

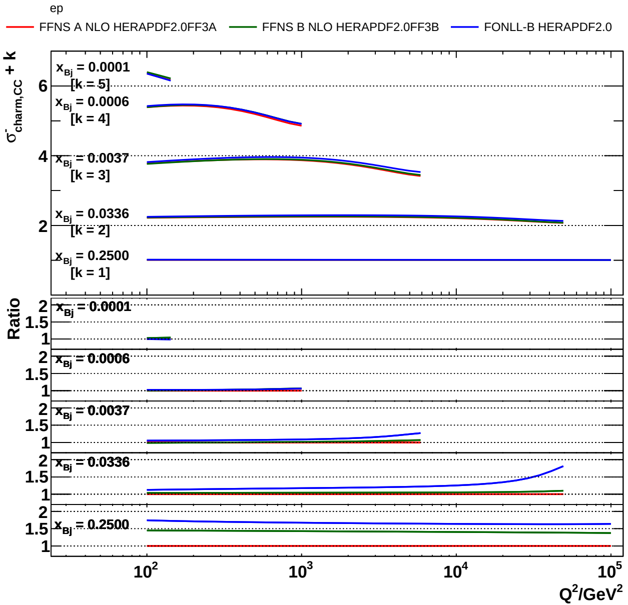

ep
FFNS A NLO HERAPDF2.0FF3A
FFNS B NLO HERAPDF2.0FF3B
FONLL-B HERAPDF2.0
$\tilde{\sigma}_{charm,CC}$ + k
x_{Bj} = 0.0001 [k = 5]
x_{Bj} = 0.0006 [k = 4]
x_{Bj} = 0.0037 [k = 3]
x_{Bj} = 0.0336 [k = 2]
x_{Bj} = 0.2500 [k = 1]
Ratio
x_{Bj} = 0.0001
x_{Bj} = 0.0006
x_{Bj} = 0.0037
x_{Bj} = 0.0336
x_{Bj} = 0.2500
10^2
10^3
10^4
10^5
Q^2/GeV^2

[1] Sayipjamal Dulat, Tie-Jiun Hou, Jun Gao, Marco Guzzi, Joey Huston, Pavel Nadolsky, Jon Pumplin, Carl Schmidt, Daniel Stump, and C. P. Yuan.
New parton distribution functions from a global analysis of quantum chromodynamics.
Phys. Rev., D93(3):033006, 2016.

[2] Richard D. Ball et al.
Parton distributions from high-precision collider data.
Eur. Phys. J., C77(10):663, 2017.

[3] S. Alekhin, J. Blmlein, S. Moch, and R. Placakyte.
Parton distribution functions, α_s, and heavy-quark masses for LHC Run II.
Phys. Rev., D96(1):014011, 2017.

[4] H. Abramowicz et al.
Combination of measurements of inclusive deep inelastic $e^{\pm}p$ scattering cross sections and QCD analysis of HERA data.
Eur. Phys. J., C75(12):580, 2015.

[5] L. A. Harland-Lang, A. D. Martin, P. Motylinski, and R. S. Thorne.
Parton distributions in the LHC era: MMHT 2014 PDFs.
Eur. Phys. J., C75(5):204, 2015.

[6] J. Alwall, R. Frederix, S. Frixione, V. Hirschi, F. Maltoni, O. Mattelaer, H. S. Shao, T. Stelzer, P. Torrielli, and M. Zaro.
The automated computation of tree-level and next-to-leading order differential cross sections, and their matching to parton shower simulations.
JHEP, 07:079, 2014.

[7] Tancredi Carli, Dan Clements, Amanda Cooper-Sarkar, Claire Gwenlan, Gavin P. Salam, Frank Siegert, Pavel Starovoitov, and Mark Sutton.
A posteriori inclusion of parton density functions in NLO QCD final-state calculations at hadron colliders: The APPLGRID Project.
Eur. Phys. J., C66:503–524, 2010.

[8] Valerio Bertone, Rikkert Frederix, Stefano Frixione, Juan Rojo, and Mark Sutton.
aMCfast: automation of fast NLO computations for PDF fits.
JHEP, 08:166, 2014.

[9] S. Alekhin, J. Blumlein, L. Caminadac, K. Lipka, K. Lohwasser, S. Moch, R. Petti, and R. Placakyte.
Determination of Strange Sea Quark Distributions from Fixed-target and Collider Data.
Phys. Rev., D91(9):094002, 2015.

[10] J. S. Conway et al.
Experimental Study of Muon Pairs Produced by 252-GeV Pions on Tungsten.
Phys. Rev., D39:92–122, 1989.

[11] B. Betev et al.
Differential Cross-section of High Mass Muon Pairs Produced by a 194-GeV/$c\pi^-$ Beam on a Tungsten Target.
Z. Phys., C28:9, 1985.
Note that the original NA10 data have since been revised; updated data are published in [26].

[12] M. Bonesini et al.
High Transverse Momentum Prompt Photon Production by π^- and π^+ on Protons at 280-GeV/c.
Z. Phys., C37:535, 1988.

[13] John M. Campbell and Richard Keith Ellis.
An Update on vector boson pair production at hadron colliders.
Phys. Rev., D60:113006, 1999.

[14] M. Botje.
QCDNUM: Fast QCD Evolution and Convolution.
Comput. Phys. Commun., 182:490–532, 2011.

[15] Karol Kovarik et al.
nCTEQ15 - Global analysis of nuclear parton distributions with uncertainties in the CTEQ framework.
Phys. Rev., D93(8):085037, 2016.

[16] P. C. Barry, N. Sato, W. Melnitchouk, and Chueng-Ryong Ji.
First Monte Carlo Global QCD Analysis of Pion Parton Distributions.
Phys. Rev. Lett., 121(15):152001, 2018.

[17] A. Abdel-Rehim et al.
Nucleon and pion structure with lattice QCD simulations at physical value of the pion mass.
Phys. Rev., D92(11):114513, 2015.
[Erratum: Phys. Rev.D93,no.3,039904(2016)].

[18] Patrick James Sutton, Alan D. Martin, Richard Goronwy Roberts, and William James Stirling.
Parton distributions for the pion extracted from Drell-Yan and prompt photon experiments.
Phys. Rev., D45:2349–2359, 1992.

[19] Chengdong Han, Hanyang Xing, Xiaopeng Wang, Qiang Fu, Rong Wang, and Xurong Chen.
Pion Valence Quark Distributions from Maximum Entropy Method, 2018.

[20] Chen Chen, Lei Chang, Craig D. Roberts, Shaolong Wan, and Hong-Shi Zong.
Valence-quark distribution functions in the kaon and pion.
Phys. Rev., D93(7):074021, 2016.

[21] C. Best, M. Gockeler, R. Horsley, Ernst-Michael Ilgenfritz, H. Perlt, Paul E. L. Rakow, A. Schafer, G. Schierholz, A. Schiller, and S. Schramm.
Pion and rho structure functions from lattice QCD.
Phys. Rev., D56:2743–2754, 1997.

[22] William Detmold, W. Melnitchouk, and Anthony William Thomas.
Parton distribution functions in the pion from lattice QCD.
Phys. Rev., D68:034025, 2003.

[23] K. Wijesooriya, P. E. Reimer, and R. J. Holt.
The pion parton distribution function in the valence region.
Phys. Rev., C72:065203, 2005.

[24] Seung-il Nam.
Parton-distribution functions for the pion and kaon in the gauge-invariant nonlocal chiral-quark model.
Phys. Rev., D86:074005, 2012.

[25] Akira Watanabe, Takahiro Sawada, and Chung Wen Kao.
Kaon quark distribution functions in the chiral constituent quark model.
Phys. Rev., D97(7):074015, 2018.

[26] W. J. Stirling and M. R. Whalley.
A Compilation of Drell-Yan cross-sections.
J. Phys., G19:D1–D102, 1993.